Early detection of high-grade squamous intraepithelial lesions in the cervix with quantitative spectroscopic imaging

Condon Lau
Jelena Mirkovic
Chung-Chieh Yu
Geoff P. O'Donoghue
Luis Galindo
Ramachandra Dasari
Antonio de las Morenas
Michael Feld
Elizabeth Stier

Early detection of high-grade squamous intraepithelial lesions in the cervix with quantitative spectroscopic imaging

Condon Lau,[a]* Jelena Mirkovic,[a]† Chung-Chieh Yu,[a]‡ Geoff P. O'Donoghue,[a]§ Luis Galindo,[a] Ramachandra Dasari,[a] Antonio de las Morenas,[b] Michael Feld,[a]‖ and Elizabeth Stier[c]
[a]Massachusetts Institute of Technology, George R. Harrison Spectroscopy Laboratory, 77 Massachusetts Avenue, Cambridge, Massachusetts 02139
[b]Boston Medical Center, Department of Pathology, One Boston Medical Center Place, Boston, Massachusetts 02118
[c]Boston Medical Center, Department of Obstetrics and Gynecology, One Boston Medical Center Place, Boston, Massachusetts 02118

Abstract. Quantitative spectroscopy has recently been extended from a contact-probe to wide-area spectroscopic imaging to enable mapping of optical properties across a wide area of tissue. We train quantitative spectroscopic imaging (QSI) to identify cervical high-grade squamous intraepithelial lesions (HSILs) in 34 subjects undergoing the loop electrosurgical excision procedure (LEEP subjects). QSI's performance is then prospectively evaluated on the clinically suspicious biopsy sites from 47 subjects undergoing colposcopic-directed biopsy. The results show the per-subject normalized reduced scattering coefficient at 700 nm (A_n) and the total hemoglobin concentration are significantly different ($p < 0.05$) between HSIL and non-HSIL sites in LEEP subjects. A_n alone retrospectively distinguishes HSIL from non-HSIL with 89% sensitivity and 83% specificity. It alone applied prospectively on the biopsy sites distinguishes HSIL from non-HSIL with 81% sensitivity and 78% specificity. The findings of this study agree with those of an earlier contact-probe study, validating the robustness of QSI, and specifically A_n, for identifying HSIL. The performance of A_n suggests an easy to use and an inexpensive to manufacture monochromatic instrument is capable of early cervical cancer detection, which could be used as a screening and diagnostic tool for detecting cervical cancer in low resource countries. © 2013 Society of Photo-Optical Instrumentation Engineers (SPIE) [DOI: 10.1117/1.JBO.18.7.076013]

Keywords: cervix; cancer; dysplasia; spectroscopy; imaging.

Paper 12521RR received Aug. 14, 2012; revised manuscript received May 31, 2013; accepted for publication Jun. 3, 2013; published online Jul. 10, 2013.

1 Introduction

Early detection is a key to reducing cervical cancer-related mortality. Cervical cancer typically is preceded by preinvasive changes known as high-grade squamous intraepithelial lesion (HSIL). The American College of Obstetrics and Gynecologists recommends that women with HSIL receive treatment of the cervical transformation zone (Tzone), typically with the loop electrosurgical excision procedure (LEEP), to prevent further progression of the disease. Therefore, for effective cervical cancer prevention, it is critical to identify the women with cervical HSIL.

The current clinical practice in cervical cancer screening involves cervical cytology, i.e., a Papanicolaou test (Pap test) for the population screening. If the Pap test result is abnormal, a direct visual examination of the cervix under magnification (colposcopy) is conducted to guide biopsy of suspicious tissues, the histopathological examination of which serves as the final diagnosis or gold standard. In the past decade, some countries have added human papillomavirus testing as an additional cervical cancer screening test for women over the age 30 (Ref. 1); however, a patient with abnormal screening is still referred for a colposcopic evaluation. Colposcopy and subsequent histopathological evaluation, even when conducted by experts, is subject to significant diagnostic variability.[2,3] A technology that can reduce diagnostic variability by using a more objective and ideally quantitative diagnostic scheme, while maintaining the ability of colposcopy to examine the entire cervix, would present a significant clinical advancement. Furthermore, if this technology is inexpensive and easy to use, it may be able to serve as a combined screening and diagnostic tool for cervical cancer prevention in developing countries, where the lack of medical infrastructure and funding have prevented implementation of a Pap test-based cancer prevention program.

Wide-area spectroscopic imaging is an extension of contact-probe optical spectroscopy developed to quantitatively detect HSIL and cancer in the cervix and other organs of the human body. Research conducted in our laboratory, as well as others, has demonstrated the ability of contact-probe spectroscopy technologies to detect dysplasia in a variety of organs including esophagus,[4,5] skin,[6] oral cavity,[7,8] breast,[9,10] and cervix.[11–17] In general, contact-probe spectroscopy has

*Present affiliation: Hong Kong University of Science and Technology, Division of Biomedical Engineering, Kowloon, Hong Kong SAR, China.
†Present affiliation: Brigham and Women's Hospital, Department of Pathology, Boston, Massachusetts 02115.
‡Present affiliation: Canon U.S.A., Inc., Optics Research Laboratory, 9030 South Rita Road, Suite 302, Tucson, Arizona 85747.
§Present affiliation: University of California, Department of Chemistry, Berkeley, California 94709.
‖Author is deceased.

Address all correspondence to: Condon Lau, Massachusetts Institute of Technology, George R. Harrison Spectroscopy Laboratory, 77 Massachusetts Avenue, Cambridge, Massachusetts 02139. Tel: (617) 2587667; Fax: (617) 2534513; E-mail: condonlau@ust.hk

demonstrated an ability to quantitatively distinguish dysplastic and cancerous cervical tissue from normal tissue, and may be more accurate than colposcopic diagnoses alone, which are subjective.

In this paper, we conduct an *in vivo* study to extend quantitative spectroscopy from contact-probe to wide-area quantitative spectroscopic imaging (QSI) for the detection of HSIL in the cervix. Imaging offers an advantage over probes in which the entire cervix can be examined in one measurement. This study follows up on a contact-probe study done by our group,[18,19] and focuses on training and prospectively evaluating QSI's ability to distinguish HSIL from non-HSIL sites on the cervical Tzone. Since the vast majority of HSILs are found in the Tzone,[20] focusing on identifying HSIL within the Tzone reduces the impact of normal anatomical variations on spectroscopy measurements and the likelihood of reporting high performance metrics for clinically less important comparisons (e.g., including significant numbers of normal ectocervix sites in the non-HSIL group).[11,18,21] We present the spectroscopic parameters observed with QSI on subjects who underwent LEEP (LEEP subjects) and women who underwent colposcopy with direct biopsy (colposcopy subjects). We normalize spectroscopy parameters to each subject individually and train QSI to distinguish HSIL from non-HSIL in the LEEP data set. The spectroscopic criteria are then applied prospectively to the colposcopy data set.

2 Materials and Methods

2.1 Instrumentation

We had previously developed a QSI system for early cancer detection with reflectance and fluorescence spectroscopy capabilities.[22] For this study, the QSI system was modified to have the functions of a digital colposcope including acquiring white-light photographs of the cervix with additional spectroscopic capabilities. In brief, colposcopic QSI illuminated a 1-mm diameter region of the cervix with visible and 337-nm light, and collected reflectance and fluorescence spectra returning from a concentric 2-mm diameter region over the visible wavelengths (400 to 700 nm). The measured spectra were fit to light propagation and fluorescence models to extract the amounts of native scatterers, absorbers, and fluorophores present.[23,24] Once the measurement was complete for one region, raster scanning was used to interrogate another 1-mm diameter region until a 2.1×2.1 cm^2 area of the cervix was examined. The total acquisition time was approximately 80 s. After the spectra were processed (offline), we obtained maps of six spectroscopy parameter: A (reduced scattering coefficient in units of mm^{-1} at 700 nm), B (wavelength dependence of reduced scattering coefficient), [Hb] (total hemoglobin concentration in units of mg/mL), α (oxygen saturation), Coll (collagen concentration in arbitrary units), and NADH (concentration of the reduced form of nicotinamide adenine dinucleotide in arbitrary units). These 21×21 pixel maps showed the value of a spectroscopy parameter at multiple points on the cervix. The QSI system compensated for the motion during the acquisition time using the white-light photographs as previously described.[22] Note that this study and earlier studies had not documented the concentrations of scatterers, absorbers, and fluorophores *in vivo* with other methods. The quantitative in QSI referred to calibration with tissue phantoms of known optical properties.

2.2 Clinical Data Acquisition

The QSI system was used to examine subjects undergoing colposcopic evaluation at the Boston Medical Center (BMC). All aspects of the study were approved by the Institutional Review Boards of the Massachusetts Institute of Technology and the BMC. Women who were pregnant, under the age of 18 or over 65, or non-English speaking were excluded from the study. Study participation was offered to all eligible subjects, and written informed consent was obtained from study participants. Five percent acetic acid was applied to the cervix to remove residual mucous and to initiate the acetowhitening effect. The QSI system was positioned at the correct orientation and distance (22.5 cm) from the subject's cervix, and data was collected. Data collection started approximately 5 min after acetic acid application. After the QSI scan, the subject underwent her scheduled procedure. Thirty-four subjects undergoing colposcopic evaluation prior to their scheduled LEEP and 47 women undergoing colposcopy with directed biopsy were recruited for the study. The 34 LEEP subjects were referred based on a prior colposcopy and subsequent HSIL histopathology diagnosis. For the colposcopy subjects, only clinically suspicious sites were biopsied; the majority of the biopsies were from the Tzone.

2.3 Histopathological Evaluation (LEEP)

Upon removal from the subject, the 12, 3, 6, and 9 o'clock positions on the squamo-columnar junction (SCJ) of the LEEP specimen were marked with color pins. Specimens were submitted to the pathology department at BMC and sectioned, stained, and evaluated per standard of care, which included sectioning the specimen into 12 pieces corresponding to the hour hands of a clock. This, combined with the four pins and the white-light photographs acquired by the QSI system, was used to correlate pathology with specific pixels on the spectroscopy parameter maps. The lead pathologist on the study (Antonio de las Morenas) classified every millimeter of all 12 sections as ectocervix, HSIL Tzone, non-HSIL Tzone, endocervix, or denuded mucosa. Note that HSIL can be further classified as cervical intraepithelial neoplasia (CIN) 2 or 3 (Ref. [25]). Non-HSIL included low-grade squamous intraepithelial lesions (LSILs) and nondysplastic tissue. No invasive cancer was observed in this study. Endocervical lesions, such as adenocarcinoma, were not evaluated in this study. The position of each millimeter along the section was measured from the SCJ, which was clearly visible on the slides and in the photographs. In sections where the SCJ was not visible in both the slides and the photographs, no position reference was recorded. For each subject, the slide(s) with the most severe disease, as identified by the lead pathologist, were also examined by two other pathologists (Christopher Crum and Sandra Cerda). They independently determined the most severe disease present on the subject (HSIL or non-HSIL). The consensus diagnosis of the most severe disease was formed from that of the majority. Only measurements from specimens where the lead pathologist's diagnosis of the most severe disease agreed with that of the consensus were used to train and evaluate QSI's ability to detect HSIL. However, measurements from all LEEP subjects were used to help determine endocervix and ectocervix (discussed below). The end result of the LEEP pathology analysis was a disease map showing the locations of HSIL on the subject (refer to Fig. 1).
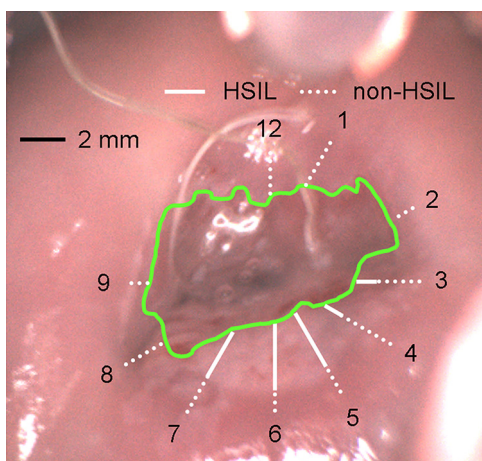
Fig. 1 High-grade squamous intraepithelial lesion (HSIL) and non-HSIL (low-grade SIL and benign) regions overlaid on a white-light photograph of the cervix. The disease state and locations were determined by loop electrosurgical excision procedure (LEEP) pathology, where the excised tissue is cut into 12 slices corresponding to the hour positions on a clock, and examined histopathologically. Solid white lines indicate regions of the cervix confirmed to have HSIL by pathology. HSIL may be present in other parts of the cervix, but these sites could not be confirmed due to denuded mucosal surfaces or finite pathology sampling. Dashed white lines indicate non-HSIL regions confirmed by pathology. Green lines indicate the squamo-columnar junction (SCJ), the boundary between endocervix and transformation zone (Tzone). No diagnosis was available at the LEEP specimen positions 10 and 11 o'clock due to denuded mucosa and part of an intrauterine device is visible.

2.4 Histopathological Evaluation (Colposcopy with Directed Biopsy)

Each biopsy specimen was submitted to pathology, where it was evaluated by three pathologists who independently rendered diagnoses of HSIL or non-HSIL. A consensus diagnosis was formed from the majority decision, and this served as the gold standard. Pathology's diagnosis for each biopsy was compared with QSI's diagnosis by using the photograph with the location of the biopsy indicated to determine the pixel on the diagnostic map closest to the biopsy site. In this fashion, we evaluated the accuracy of QSI, used as an adjunct to colposcopy, by providing a diagnosis of HSIL or non-HSIL at clinically suspicious sites.

2.5 Data Analysis (LEEP)

Spectroscopy parameters, measured from HSIL and non-HSIL pixels in the Tzones of LEEP subjects, were selected by correlating the disease maps to the spectroscopy parameter maps. This was accomplished by identifying the 12, 3, 6, and 9 o'clock positions on the SCJ of each subject using the white-light photographs acquired by the QSI system.[22] Since the photographs were acquired simultaneously with the parameter maps, each millimeter on the disease map was matched with the pixels of the parameter maps (refer to Fig. 1). We did not include the effects of possible specimen shrinkage following fixation.[26] Pixels corresponding to denuded mucosa or sections without a visible SCJ were not included in the subsequent analyses.

Spectroscopy parameters measured from ectocervix pixels on all subjects were used for normalizing spectroscopy parameter maps. There are normal inter-subject variations in tissue properties due to factors such as age and menstrual cycle.[14,27–29] These are reflected in spectroscopy parameters, and may confound contrast due to disease.[28,30] We normalized all spectroscopy parameter maps per subject to counteract the impact of normal variations. Normalization for each parameter was done by dividing the value at each pixel of the parameter map by the average value of the parameter measured from pixels corresponding to normal ectocervix. Normalized parameters were denoted by a subscript n (A versus A_n). A similar normalization procedure was applied in our recent contact-probe study, and yielded improved distinction of HSIL from non-HSIL.[19]

To train QSI to identify ectocervix pixels for normalization, the A and Coll values from colposcopically defined ectocervix and nonectocervix pixels were used to form the likelihood functions in a Bayesian analysis. Schomacker et al. previously observed that normal squamous can be distinguished from CIN 2 and 3 using fluorescence spectra.[31] We used the number of ectocervix pixels and the total number of cervix pixels (total number of pixels covering the cervices of the LEEP subject including ectocervix pixels) to form the prior probability. The Bayesian analysis was applied to the spectroscopy data from all LEEP subjects to identify ectocervix pixels given the local A and Coll values (posterior probability greater than 0.5). For each subject, all such ectocervix pixels surrounded by at least eight other such ectocervix pixels (continuity criterion) were used as the spectroscopy parameter normalization region. Normalized spectroscopy parameter maps of each subject were formed by dividing each regular parameter map by the average value of the corresponding parameter in ectocervix pixels of the subject. Note that pixels not chosen for normalization may span the endocervix, Tzone, and ectocervix. Choosing pixels for normalization does not imply the remaining pixels define the Tzone.

2.6 Data Analysis (Colposcopy)

The Bayesian analysis and continuity criterion were also applied to the spectroscopy data from all colposcopy subjects to identify ectocervix pixels. The likelihood functions and prior probability were obtained from the LEEP data. Normalized spectroscopy parameter maps of each subject were formed by dividing each regular parameter map by the average value of the corresponding parameter in ectocervix pixels of the subject.

3 Results

A total of 34 LEEP subjects and 47 colposcopy subjects were recruited for this study. The study participants consisted of 43 self-identified blacks, 19 whites, 16 Hispanic/Latinos, 2 Asians, and 1 other. Their ages had a mean of 31.3 years and a standard deviation of 9.7 years. Twenty of the subjects had referral cytology of atypical squamous cells of undetermined significance (ASCUS), three had atypical squamous cells cannot rule out a high-grade lesion (ASC-H), 36 had LSIL, 18 had HSIL, and four had other. Among the LEEP subjects, two had referral cytology negative for intraepithelial lesion or malignancy, seven had ASCUS, one had ASC-H, 12 had LSIL, 10 had HSIL, and two had unknown. Since this study is the initial clinical deployment of the QSI system, the first four LEEP subjects were required to optimize the equipment and to repair problems. Spectroscopic results from the remaining 30 LEEP subjects are presented. The lead pathologist's diagnosis agreed with that of the consensus in 25 of the LEEP subjects, and these are used to train QSI to identify HSIL. All 30 LEEP subjects

Table 1 The number of subjects undergoing different numbers of colposcopically directed biopsies. All biopsies were performed due to clinical need only. Other refers to subjects without spectroscopy data due to instrument problems, and their pathology results were not recorded in the study. Note that there was no spectroscopy data at 10 of the biopsy sites due to blood, specular reflection, or the site not being covered by the scan. No pathology data was available at four of the biopsy sites due to specimen damage. This resulted in the 67 biopsy sites with spectroscopy data in the study.

# of biopsies	0	1	2	3	4	Other
# of subjects	5	16	10	11	3	2

Table 2 The number of subjects undergoing different numbers of colposcopically directed biopsies that were histopathologically diagnosed as high-grade squamous intraepithelial lesion (HSIL). No spectroscopy data was available at two of the HSIL-biopsy sites. This resulted in the 16 HSIL-biopsy sites with spectroscopy data in the study.

# of HSIL biopsies	0	1	2	3	4	Other
# of subjects	34	6	4	0	1	2

with spectroscopy measurements were used to identify ectocervix. Eighteen of the 25 LEEP subjects had histopathologically diagnosed HSIL. The colposcopy study yielded 16 HSIL and 51 non-HSIL biopsies. Table 1 shows the number of subjects undergoing different numbers of colposcopically directed biopsies. Table 2 shows the number of subjects undergoing different numbers of colposcopically directed biopsies which were

histopathologically diagnosed as HSIL. HSIL biopsies were obtained from 11 of the colposcopy subjects.

QSI measures tissue spectroscopic properties at multiple sites across the cervix. Figure 2 shows all six spectroscopy parameter maps measured from a representative cervix. The dark slit near the center is the cervical os, the opening of the endocervical canal. Away from the os near the edge of the cervix is the ectocervix, which is characterized by higher scattering [upper and lower portions of Fig. 2(a)]. Between the endocervix and ectocervix, spectroscopy parameters transition from columnar to squamous values. The region between the endocervix and ectocervix is the Tzone. In general, the Tzone has lower A, lower B, higher [Hb], lower α, lower Coll, and higher NADH than ectocervix.

Spectroscopy parameters in this study are normalized by their respective average values across ectocervix pixels of the same subject. Figure 3 shows the six box plots of normalized parameters measured from all HSIL and non-HSIL pixels of the LEEP subjects. HSIL pixels exhibit considerably lower scattering (A_n) than non-HSIL pixels [Fig. 3(a)]. The p-value of this difference, computed using the two-tailed t-test, is 0 (beyond computer precision). HSIL also has slightly lower B_n [$p > 0.05$, Fig. 3(b)], α_n [$p > 0.05$, Fig. 3(d)], and $Coll_n$ [$p > 0.05$, Fig. 3(e)], and slightly higher [Hb]$_n$ [$p < 0.01$, Fig. 3(c)] and $NADH_n$ [$p > 0.05$, Fig. 3(f)] than non-HSIL. However, these differences are small when compared with the A_n difference. Applying a threshold of $A_n < 0.83$ (HSIL) and $A_n > 0.83$ (non-HSIL) on the boxplot of Fig. 3(a), HSIL can be distinguished from non-HSIL with 89% sensitivity and 83% specificity. Note that these two values are reported for all HSIL and non-HSIL pixels. The 0.83 A_n threshold maximizes the sum of sensitivity and specificity in the LEEP data set. Therefore, QSI can retrospectively distinguish HSIL from
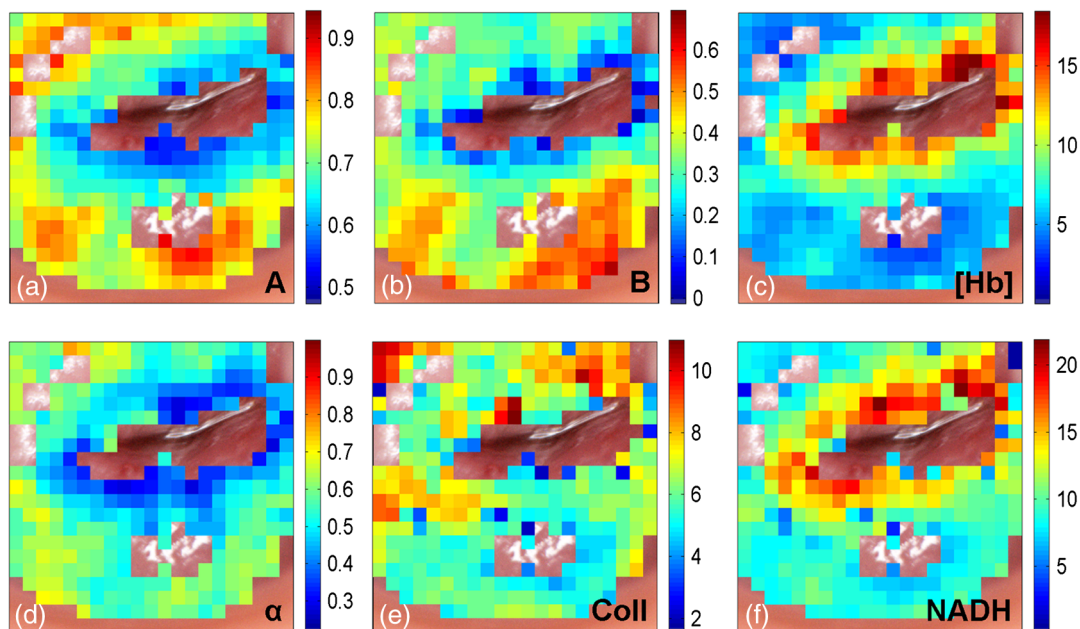

Fig. 2 Spectroscopy parameter maps acquired by quantitative spectroscopic imaging (QSI) overlaid on a white-light photograph of a cervix. (a) A, reduced scattering coefficient at 700 nm (mm^{-1}). (b) B, wavelength dependence of reduced scattering coefficient. (c) [Hb], total hemoglobin concentration (mg/mL). (d) α, oxygen saturation (%). (e) Coll, collagen concentration (a.u.). (f) NADH, concentration of reduced form of nicotinamide adenine dinucleotide (a.u.). Pixels with no spectroscopy data due to the presence of specular reflection, motion, acute tissue angle relative to QSI system, or noncervical substances are uncolored in the parameter maps. Note that specular reflection observed in the white-light photographs is not necessarily sites of specular reflection for spectroscopy measurements. A portion of the speculum (bottom of photograph) is visible.
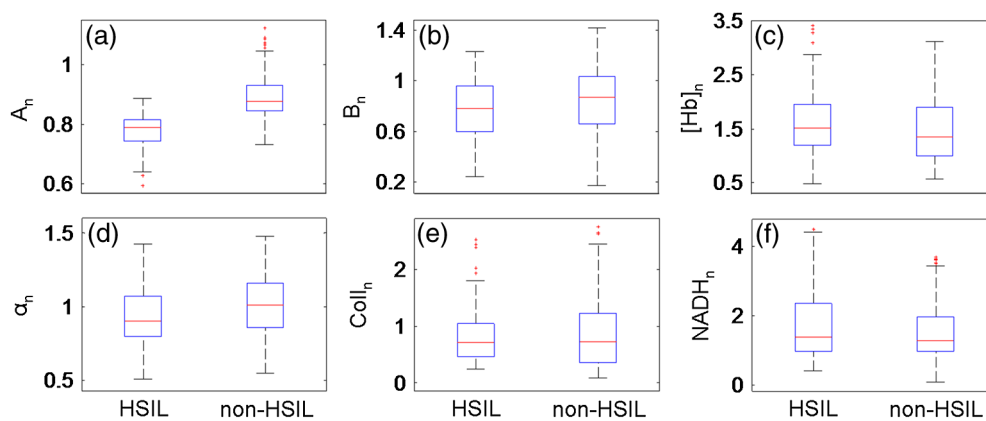
Fig. 3 Box plots of normalized spectroscopy parameters measured from HSIL and non-HSIL pixels in the excised region of the LEEP subjects. Normalization was performed by dividing spectroscopy parameters by their respective average values across ectocervix pixels of the same subject. (a) A_n, normalized A. (b) B_n, normalized B. (c) $[Hb]_n$, normalized $[Hb]$. (d) α_n, normalized α. (e) $Coll_n$, normalized Coll. (f) $NADH_n$, normalized NADH. The horizontal center line is the median and the lower and upper edges of the rectangular box indicate the 25th and 75th percentiles, respectively. The horizontal lines at the ends of the dashed vertical line indicate the extent of the data, and the crosses indicate outliers.
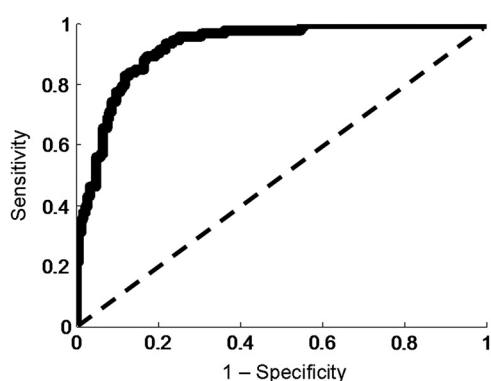

Fig. 4 Receiver operator characteristic (ROC) curve (solid line) for distinguishing HSIL from non-HSIL pixels in the LEEP subjects. Only A_n was used in the analysis. The dashed line indicates the line of chance.

Fig. 5 Mean reflectance (a) and fluorescence (b) spectra acquired from the clinically suspicious biopsy sites of colposcopy subjects. Solid lines indicate non-HSIL sites, and dashed lines indicate HSIL sites. Note that these spectra are not "normalized" like the spectroscopy parameter maps.

non-HSIL in LEEP subjects with 89% sensitivity and 83% specificity, which is in good agreement with an earlier contact-probe study.[19]

Figure 4 shows the entire receiver operator characteristic (ROC) curve for distinguishing HSIL from non-HSIL in the LEEP subjects computed using A_n only. The ROC curve shows different retrospective sensitivities and specificities that can be achieved with different A_n thresholds (the $A_n = 0.83$ threshold is included in the ROC curve). The area under the ROC curve, a measure of QSI's ability to distinguish HSIL from non-HSIL, is 0.93 (1.0 is perfect distinction, and 0.5 is equivalent to chance).

Figure 5 shows the mean reflectance and fluorescence spectra acquired from clinically suspicious biopsy sites of colposcopy subjects. The differences between HSIL and non-HSIL spectra are small. Note that these spectra are not "normalized" like the spectroscopy parameter maps. QSI with an A_n threshold of 0.83 was then applied prospectively to the biopsy sites to distinguish HSIL from non-HSIL. Note that both the A_n threshold and the A and Coll values for identifying ectocervix were chosen from the LEEP data only. Table 3 shows the 13 true positives, 11 false positives, 40 true negatives, and 3 false negatives. QSI can prospectively distinguish HSIL from non-HSIL in colposcopy
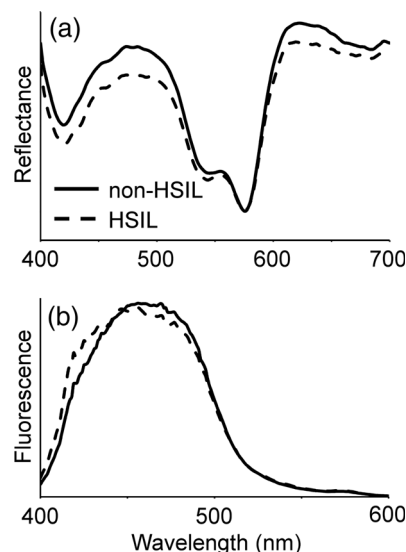
subjects with 81% sensitivity and 78% specificity. This is a measure of QSI's performance identifying HSIL when used as an adjunct to colposcopy. Combining colposcopy with spectroscopy would require 13 (true positives) +11 (false positives) biopsies be taken from the 47 colposcopy subjects. This comes to 0.51 biopsies per subject.

Table 3 Prospective evaluation of quantitative spectroscopic imaging's (QSI's) ability to distinguish HSIL from non-HSIL in the biopsy sites of colposcopy subjects. The rows are QSI's diagnoses, and the columns are consensus pathology's classifications. There are 13 true positives, 11 false positives, 3 false negatives, and 40 true negatives.

	HSIL biopsy	Non-HSIL biopsy
HSIL QSI ($A_n < 0.83$)	13	11
Non-HSIL QSI ($A_n > 0.83$)	3	40

4 Discussion

The results presented in this paper demonstrate QSI's ability to measure cervical tissue properties *in vivo*. This measurement of reflectance and fluorescence properties is equivalent to several hundred contact-probe measurements (Fig. 2), and can be completed in a relatively short period of time. Spectroscopy parameter maps measured from the cervix show that the Tzone has lower A, lower B, higher [Hb], lower α, lower Coll, and higher NADH than ectocervix. We also find HSIL pixels exhibit considerably lower normalized A than non-HSIL pixels in the LEEP subjects, while other normalized parameters exhibit relatively little difference between the disease states. QSI can retrospectively distinguish HSIL from non-HSIL in the LEEP subjects with 89% sensitivity, 83% specificity, and area under ROC curve = 0.93 using A_n alone. Using the thresholds obtained from the LEEP data set, QSI can prospectively distinguish HSIL from non-HSIL in colposcopy subjects with 81% sensitivity and 78% specificity.

Previous efforts have been made to combine spectroscopy with wide-area imaging in the cervix[32–43] to enable wide-area surveillance as is done in colposcopy. For example, Milbourne et al.[32] and Park et al.[36] conducted three color reflectance and fluorescence spectroscopic imagings, and observed that dysplastic tissue emits slightly different colors than normal tissue when excited with ultraviolet or blue excitation light. Alvarez et al. conducted a randomized trial using the LUMA cervical imaging system to determine if combining reflectance and fluorescence spectroscopic imaging with colposcopy on subjects referred for colposcopy would increase HSIL detection.[33] They determined that combining spectroscopy with colposcopy improved the true positive rate of HSIL detection among subjects with ASC or LSIL cytology by 26% over colposcopy alone. However, this benefit came at the expense of a 33% increase in the number of biopsies taken from those subjects. Huh et al. similarly observed that spectroscopy+colposcopy increased the detection of HSIL by 25% among women with ASC/LSIL cytology.[43]

QSI differs from previous spectroscopic imaging techniques in two significant ways. First, QSI is the imaging implementation of quantitative spectroscopy, which means it measures tissue properties by using biophysical models of light propagation to extract information about tissue scatterers, absorbers, and fluorophores from the measured spectra.[22–24] Modeling allows QSI to directly measure tissue structural and biochemical changes associated with disease. Without modeling, spectral measurements may vary significantly with instrument configuration.[44] Several contact-probe spectroscopy studies have also used biophysical modeling to measure tissue changes.[11,13,21,45,46] Understanding these changes will allow knowledge obtained from QSI studies done with one instrument implementation to be transferred to another implementation, and potentially facilitates extending QSI to detect early cancer in other body organs. Second, QSI uses narrow-field illumination, while other systems use wide-field illumination. Narrow-field illumination results in a smaller sampling volume at each pixel, similar to the difference between confocal and bright field microscopy, and thus, likely allows QSI to detect smaller dysplasia.

In addition to biophysical modeling, our proposed QSI diagnostic approach specifically helps to address the effects of inter-subject variability. Normalized spectroscopy parameters that highlight contrast within the same subject are used, because diagnosis with the regular parameters can couple intra- and inter-subject contrast. Inter-subject contrast may be due to normal cervical variations, such as age and menopausal status, or time after acetic acid application.[11,14,28,29,47] Normalization was also used successfully by Mirkovic et al. to distinguish HSIL from non-HSIL with a contact-probe implementation of quantitative spectroscopy.[19] In that study, the A_n parameter was obtained by dividing spectroscopy parameters measured at clinically suspicious sites (biopsied after measurement) by the respective parameters measured at normal ectocervix sites. The authors reported retrospective sensitivity and specificity of 89% and 79%, respectively, distinguishing HSIL from non-HSIL at the biopsy sites of colposcopy subjects.

This study focuses on distinguishing HSIL from non-HSIL in the cervical Tzone, which reduces the impact of normal anatomical variations on spectroscopy parameters and also the likelihood of reporting high performance metrics for clinically less important comparisons (e.g., distinguishing HSIL from normal ectocervix).[18] The changes in A_n observed with HSIL are likely due to QSI measuring changes in stromal density that occur due to degradation by matrix metalloproteinases.[48] This can reduce the amount of scattering from the stroma, which has significant influence on tissue reflectance spectra.[49] Several earlier studies have observed a similar trend in their data. Nordstrom et al. reported that reflectance spectroscopy alone helped to distinguish HSIL from nondysplastic Tzone, and fluorescence measurements were not effective.[50] Similarly, Mirabal et al. noted a decrease in tissue reflectivity with the severity of dysplasia.[51] However, because these authors did not conduct quantitative spectroscopy, they could not separate the scattering and absorption contributions to reflectance, as we did in this paper, which allows us to observe the importance of scattering measurements alone.

Acetic acid was applied to the cervix in this study prior to QSI. The subsequent aceto-whitening changes would be expected to increase scattering in HSIL relative to non-HSIL. However, this study observed lower scattering (i.e., A_n) in HSIL. There are several potential reasons for the discrepancy. In this study, QSI started approximately 5 min after acetic acid application. The most optically apparent and dynamic aceto-whitening changes occur within five minutes of application.[38,40] The remaining aceto-whitening changes likely affect reflectance at short wavelengths more than at the long wavelengths, where A_n is measured. Wu and Qu observed that backscattering by cell monolayers increased after acetic acid application, more so at short than at long wavelengths.[52] *In vivo*, increased backscattering may decrease the amount of short wavelength light penetrating the epithelium and reaching the blood vessels, thus increasing reflectance. This effect is less pronounced at long wavelengths, where A_n is measured, because hemoglobin absorption is minimal. Due to the above reasons, aceto-whitening is unlikely to be contradictory to the results of this study.

This study prospectively evaluates QSI's ability to distinguish HSIL from non-HSIL at the clinically suspicious biopsy sites of colposcopy subjects. One of the potential applications of this research is an optical system that is used with standard colposcopy to identify biopsy sites. Compared with colposcopy alone, such a combined system may reduce the number of biopsies required to sample the cervix without considerably reducing HSIL detection. Future studies will be performed to determine the number of biopsies called by the combined system, the number of HSIL sites detected, and the number of subjects with HSIL detected. A HSIL pathology result was chosen as the

threshold in this study, because it is the current threshold for treatment (e.g., by LEEP). An alternative threshold is a CIN 3 pathology result. In this study, CIN 2 and 3 pathology results were grouped together as HSIL pathology. However, if the system were tuned to identify only CIN 3 pathology, there would be a significant likelihood of missing biologic CIN 3. This is because a CIN 2 pathology result is often misclassified as biologic CIN 3 (Ref. 53). Therefore, HSIL pathology is the more suitable threshold for this QSI study.

The QSI system described so far in this study is not suitable for use in a low-resource setting. However, the finding that measuring the reduced scattering coefficient at one wavelength can distinguish HSIL from non-HSIL permits the design of a significantly simpler, faster, and less-expensive optical system for cervical dysplasia detection. The simple optical system's simplicity may facilitate its use as a screening and diagnostic tool in low-resource developing countries, which lack the medical infrastructure for implementing cervical cancer screening programs. This system, potentially based on a red laser pointer and an optical power meter, could cost very little to manufacture and would be easy to use. The system can likely be operated with battery power, and will not require computer control. A properly designed container should shield the optics from water, dust, and dirt. The simple optical system will also be a valuable addition to a standard colposcope in the developed countries.

The operator of the simple optical system will be trained to identify ectocervix sites for normalization. Such sites are typically located far from the SCJ and Tzone. Study is required to determine visual features for identifying normalization sites, although we expect the features to be similar to those of ectocervix as viewed through a magnifying glass. Identifying normalization sites should require less training than performing standard colposcopy. Also note that the simple system will likely be employed in low-resource settings without a pathology lab. Therefore, any subject with a low A_n measurement would be treated on the spot without taking biopsies. Whether or not this leads to an excessive number of unnecessary treatments will be investigated. Sampling strategies will be devised to optimize the balance between sensitivity and specificity.

References

1. D. Saslow et al., "American Cancer Society, American Society for Colposcopy and Cervical Pathology, and American Society for Clinical Pathology screening guidelines for the prevention and early detection of cervical cancer," *CA Cancer J. Clin.* **62**(3), 147–172 (2012).
2. M. Sideri et al., "Interobserver variability of colposcopic interpretations and consistency with final histologic results," *J. Low. Genit. Tract Dis.* **8**(3), 212–216 (2004).
3. M. H. Stoler et al., "Interobserver reproducibility of cervical cytologic and histologic interpretations: realistic estimates from the ASCUS-LSIL Triage Study," *JAMA* **285**(11), 1500–1505 (2001).
4. I. Georgakoudi et al., "Fluorescence, reflectance, and light-scattering spectroscopy for evaluating dysplasia in patients with Barrett's esophagus," *Gastroenterology* **120**(7), 1620–1629 (2001).
5. M. Panjehpour et al., "Spectroscopic diagnosis of esophageal cancer: new classification model, improved measurement system," *Gastrointest. Endosc.* **41**(6), 577–581 (1995).
6. L. Brancaleon et al., "*In vivo* fluorescence spectroscopy of nonmelanoma skin cancer," *Photochem. Photobiol.* **73**(2), 178–183 (2001).
7. D. C. de Veld et al., "Autofluorescence and diffuse reflectance spectroscopy for oral oncology," *Lasers Surg. Med.* **36**(5), 356–364 (2005).
8. M. G. Muller et al., "Spectroscopic detection and evaluation of morphologic and biochemical changes in early human oral carcinoma," *Cancer* **97**(7), 1681–1692 (2003).
9. J. Q. Brown et al., "Quantitative optical spectroscopy: a robust tool for direct measurement of breast cancer vascular oxygenation and total hemoglobin content *in vivo*," *Cancer Res.* **69**(7), 2919–2926 (2009).
10. Z. Volynskaya et al., "Diagnosing breast cancer using diffuse reflectance spectroscopy and intrinsic fluorescence spectroscopy," *J. Biomed. Opt.* **13**(2), 024012 (2008).
11. I. Georgakoudi et al., "Trimodal spectroscopy for the detection and characterization of cervical precancers *in vivo*," *Am. J. Obstet. Gynecol.* **186**(3), 374–382 (2002).
12. S. K. Chang et al., "Combined reflectance and fluorescence spectroscopy for *in vivo* detection of cervical pre-cancer," *J. Biomed. Opt.* **10**(2), 024031 (2005).
13. J. R. Mourant et al., "*In vivo* light scattering measurements for detection of precancerous conditions of the cervix," *Gynecol. Oncol.* **105**(2), 439–445 (2007).
14. J. R. Mourant et al., "Detection of cervical intraepithelial neoplasias and cancers in cervical tissue by *in vivo* light scattering," *J. Low. Genit. Tract Dis.* **13**(4), 216–223 (2009).
15. S. B. Cantor et al., "Accuracy of optical spectroscopy for the detection of cervical intraepithelial neoplasia: testing a device as an adjunct to colposcopy," *Int. J. Cancer* **128**(5), 1151–1168 (2011).
16. V. T. Chang et al., "Visible light optical spectroscopy is sensitive to neovascularization in the dysplastic cervix," *J. Biomed. Opt.* **15**(5), 057006 (2010).
17. E. M. Kanter et al., "Application of Raman spectroscopy for cervical dysplasia diagnosis," *J. Biophoton.* **2**(1–2), 81–90 (2009).
18. J. Mirkovic et al., "Effect of anatomy on spectroscopic detection of cervical dysplasia," *J. Biomed. Opt.* **14**(4), 044021 (2009).
19. J. Mirkovic et al., "Detecting high-grade squamous intraepithelial lesions in the cervix with quantitative spectroscopy and per-patient normalization," *Biomed. Opt. Express* **2**(10), 2917–2925 (2011).
20. D. Ferris et al., *Modern Colposcopy: Textbook and Atlas*, American Society for Colposcopy and Cervical Pathology, Dubuque, Iowa (2004).
21. J. R. Mourant et al., "*In vivo* light scattering for the detection of cancerous and precancerous lesions of the cervix," *Appl. Opt.* **48**(10), D26–D35 (2009).
22. C. C. Yu et al., "Quantitative spectroscopic imaging for non-invasive early cancer detection," *Opt. Express* **16**(20), 16227–16239 (2008).
23. G. Zonios et al., "Diffuse reflectance spectroscopy of human adenomatous colon polyps *in vivo*," *Appl. Opt.* **38**(31), 6628–6637 (1999).
24. M. G. Muller et al., "Intrinsic fluorescence spectroscopy in turbid media: disentangling effects of scattering and absorption," *Appl. Opt.* **40**(25), 4633–4646 (2001).
25. T. M. Darragh et al., "The lower anogenital squamous terminology standardization project for HPV-associated lesions: background and consensus recommendations from the College of American Pathologists and the American Society for Colposcopy and Cervical Pathology," *Arch. Pathol. Lab. Med.* **136**(10), 1266–1297 (2012).
26. P. L. Hsiung, P. R. Nambiar, and J. G. Fujimoto, "Effect of tissue preservation on imaging using ultrahigh resolution optical coherence tomography," *J. Biomed. Opt.* **10**(6), 064033 (2005).
27. C. K. Brookner et al., "Autofluorescence patterns in short-term cultures of normal cervical tissue," *Photochem. Photobiol.* **71**(6), 730–736 (2000).
28. J. A. Freeberg et al., "Fluorescence and reflectance device variability throughout the progression of a phase II clinical trial to detect and screen for cervical neoplasia using a fiber optic probe," *J. Biomed. Opt.* **12**(3), 034015 (2007).

29. S. K. Chang et al., "Fluorescence spectroscopy for cervical precancer detection: is there variance across the menstrual cycle?," *J. Biomed. Opt.* **7**(4), 595–602 (2002).

30. E. Vargis et al., "Sensitivity of Raman spectroscopy to normal patient variability," *J. Biomed. Opt.* **16**(11), 117004 (2011).

31. K. T. Schomacker et al., "Novel optical detection system for *in vivo* identification and localization of cervical intraepithelial neoplasia," *J. Biomed. Opt.* **11**(3), 34009 (2006).

32. A. Milbourne et al., "Results of a pilot study of multispectral digital colposcopy for the *in vivo* detection of cervical intraepithelial neoplasia," *Gynecol. Oncol.* **99**(3 Suppl 1), S67–S75 (2005).

33. R. D. Alvarez and T. C. Wright, and Optical Detection Group, "Effective cervical neoplasia detection with a novel optical detection system: a randomized trial," *Gynecol. Oncol.* **104**(2), 281–289 (2007).

34. T. DeSantis et al., "Spectroscopic imaging as a triage test for cervical disease: a prospective multicenter clinical trial," *J. Low. Genit. Tract Dis.* **11**(1), 18–24 (2007).

35. D. G. Ferris et al., "Multimodal hyperspectral imaging for the noninvasive diagnosis of cervical neoplasia," *J. Low. Genit. Tract Dis.* **5**(2), 65–72 (2001).

36. S. Y. Park et al., "Automated image analysis of digital colposcopy for the detection of cervical neoplasia," *J. Biomed. Opt.* **13**(1), 014029 (2008).

37. J. Louwers et al., "Dynamic spectral imaging colposcopy: higher sensitivity for detection of premalignant cervical lesions," *BJOG* **118**(3), 309–318 (2011).

38. T. Wu et al., "Clinical study of quantitative diagnosis of early cervical cancer based on the classification of acetowhitening kinetics," *J. Biomed. Opt.* **15**(2), 026001 (2010).

39. B. W. Pogue, M. A. Mycek, and D. Harper, "Image analysis for discrimination of cervical neoplasia," *J. Biomed. Opt.* **5**(1), 72–82 (2000).

40. B. W. Pogue et al., "Analysis of acetic acid-induced whitening of high-grade squamous intraepithelial lesions," *J. Biomed. Opt.* **6**(4), 397–403 (2001).

41. R. D. Alvarez and T. C. Wright Jr., and Optical Detection Group, "Increased detection of high-grade cervical intraepithelial neoplasia utilizing an optical detection system as an adjunct to colposcopy," *Gynecol. Oncol.* **106**(1), 23–28 (2007).

42. W. K. Huh et al., "Optical detection of high-grade cervical intraepithelial neoplasia *in vivo*: results of a 604-patient study," *Am. J. Obstet. Gynecol.* **190**(5), 1249–1257 (2004).

43. W. K. Huh, "Optical detection of cervical neoplasia: results from an internally-controlled multicenter study," in *4th Int. Conf. on Cervical Cancer in 2005*, Houston, Texas (2005).

44. S. C. Gebhart, S. K. Majumder, and A. Mahadevan-Jansen, "Comparison of spectral variation from spectroscopy to spectral imaging," *Appl. Opt.* **46**(8), 1343–1360 (2007).

45. S. K. Chang et al., "Model-based analysis of clinical fluorescence spectroscopy for *in vivo* detection of cervical intraepithelial dysplasia," *J. Biomed. Opt.* **11**(2), 024008 (2006).

46. C. Redden Weber et al., "Model-based analysis of reflectance and fluorescence spectra for *in vivo* detection of cervical dysplasia and cancer," *J. Biomed. Opt.* **13**(6), 064016 (2008).

47. C. Brookner et al., "Effects of biographical variables on cervical fluorescence emission spectra," *J. Biomed. Opt.* **8**(3), 479–483 (2003).

48. I. Pavlova et al., "Microanatomical and biochemical origins of normal and precancerous cervical autofluorescence using laser-scanning fluorescence confocal microscopy," *Photochem. Photobiol.* **77**(5), 550–555 (2003).

49. D. Arifler et al., "Spatially resolved reflectance spectroscopy for diagnosis of cervical precancer: Monte Carlo modeling and comparison to clinical measurements," *J. Biomed. Opt.* **11**(6), 064027 (2006).

50. R. J. Nordstrom et al., "Identification of cervical intraepithelial neoplasia (CIN) using UV-excited fluorescence and diffuse-reflectance tissue spectroscopy," *Lasers Surg. Med.* **29**(2), 118–127 (2001).

51. Y. N. Mirabal et al., "Reflectance spectroscopy for *in vivo* detection of cervical precancer," *J. Biomed. Opt.* **7**(4), 587–594 (2002).

52. T. T. Wu and J. Y. Qu, "Assessment of the relative contribution of cellular components to the acetowhitening effect in cell cultures and suspensions using elastic light-scattering spectroscopy," *Appl. Opt.* **46**(21), 4834–4842 (2007).

53. P. E. Castle et al., "The relationship of community biopsy-diagnosed cervical intraepithelial neoplasia grade 2 to the quality control pathology-reviewed diagnoses: an ALTS report," *Am. J. Clin. Pathol.* **127**(5), 805–815 (2007).